# Mobility of Functionalized Quantum Dots and a Model Polystyrene Nanoparticle in Saturated Quartz Sand and Loamy Sand

**ARTICLE** *in* ENVIRONMENTAL SCIENCE & TECHNOLOGY · MARCH 2012

Impact Factor: 5.33 · DOI: 10.1021/es2045458 · Source: PubMed



**2 AUTHORS:**

Ivan Quevedo
Universidad Iberoamericana Ciudad de México
**13** PUBLICATIONS **483** CITATIONS
SEE PROFILE

Nathalie Tufenkji
McGill University
**122** PUBLICATIONS **3,611** CITATIONS
SEE PROFILE

Environmental Science & Technology

Article

pubs.acs.org/est

# Mobility of Functionalized Quantum Dots and a Model Polystyrene Nanoparticle in Saturated Quartz Sand and Loamy Sand

Ivan R. Quevedo[†] and Nathalie Tufenkji*[,†]

[†]Department of Chemical Engineering, McGill University, Montreal, Quebec H3A 2B2, Canada

Supporting Information

**ABSTRACT:** Quantum dots (QDs) are one example of engineered nanoparticles (ENPs) with demonstrated toxic effects. Yet, little is known about the behavior of QDs in the natural environment. This study assessed the transport of two commercial carboxylated QDs (CdTe and CdSe) and carboxylated polystyrene latex (*n*PL) as a model nanoparticle using saturated laboratory-scale columns. The influence of solution ionic strength (IS) and cation type ($K^+$ or $Ca^{2+}$) on the transport potential of these ENPs was examined in two granular matrices − quartz sand and loamy sand. The retention of all three particles was generally low in the quartz sand columns within the range of studied IS (0.1−100 mM) for the monovalent salt (KCl). In contrast, the retention of the three ENPs in the quartz sand was significant in the presence of 10 mM $Ca^{2+}$. Moreover, ENP attachment efficiencies ($\alpha$) were enhanced by at least 1 order of magnitude in columns packed with loamy sand (for IS between 0.1−10 mM KCl). Although all three ENPs used here are carboxylated, they differ in the type of surface coating (e.g., choice of polymers or polyelectrolytes). Regardless of the surface coatings, the three ENPs exhibit comparable mobility in the quartz sand. However, the ENPs demonstrate variable transport potential in loamy sand suggesting that differences in the binding affinities of surface-modified ENPs for specific soil constituents can play a key role in the fate of ENPs in soils.

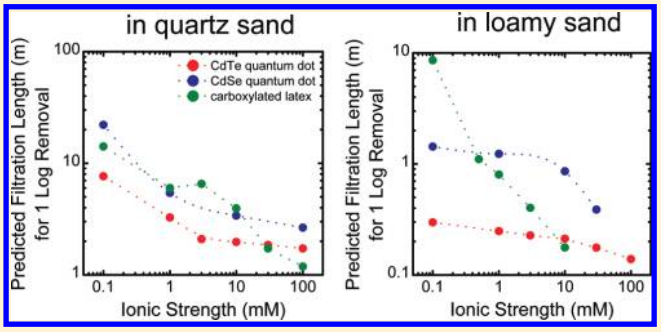


## INTRODUCTION

It is expected that by the year 2020, the equivalent of six trillion U.S. dollars in consumer products will incorporate nanomaterials.[1] Many economic and societal benefits are expected from nanotechnology, but there are likely risks to human and ecosystem health because engineered nanoparticles (ENPs) are generally more reactive and potentially more persistent than bulk materials with similar chemical composition.[2,3]

Quantum dots (QDs) are one example of ENPs that exhibit distinctive optical and electrical characteristics[4,5] due to their composition and small size (typical diameters are between 2 and 100 nm). Because QDs have excellent fluorescent properties and narrow emission spectra compared to other fluorophores, they are particularly useful in the development of transistors, solar cells, lasers, medical imaging, and computing systems.[6−8] Typically, QDs are composed of a binary alloy of semiconducting metals (e.g., CdTe, CdSe, InAs, InP) protected by a shell (ZnS, CdS), which is coated with polymers or polyelectrolytes to make them dispersible in aqueous media.[4,9] Although some promising silicon-based QDs are under development,[10,11] current commercial QDs contain toxic heavy metals, and several studies demonstrate their cytotoxic effects on living organisms.[12−14] QDs may be introduced into the natural environment via waste streams from industries that synthesize or use them and via clinical and research facilities. After their release into aquatic or soil ecosystems or wastewater treatment facilities, the potential toxicological risks of QDs will be directly related to their mobility and transformation within these environments.[15−17]

The transport and fate of a wide range of ENPs in systems representative of natural subsurface environments or engineered (deep-bed) granular filtration processes have been examined in a number of laboratory investigations.[18] In general, studies conducted with various surface-modified or coated ENPs suggest they possess greater mobility in water-saturated granular matrices than their bare counterparts.[19−24] For instance, several researchers have examined the transport potential of surface-modified zero-valent iron nanoparticles (nZVI) in model subsurface environments, demonstrating the effective electrosteric stabilizing efficiency of various polyelectrolytes or organic coatings.[19,22−24] However, the variability in the experimental approach and conditions used in each study complicates the generalization of such findings to a broader range of ENPs. Moreover, only a limited number of studies[25−27] have addressed the transport potential of QDs in subsurface environments. For instance, Torkzaban et al.[26] studied the retention of a carboxylated CdTe QD in water

Received: December 18, 2011
Revised: March 15, 2012
Accepted: March 19, 2012
Published: March 19, 2012

saturated sand packed columns as a function of solution IS (in NaCl solution). They observed little deposition of this QD in ultrapure quartz sand, but the retention was greatly enhanced in the presence of impurities on the sand surface and in columns packed with goethite-coated sand. Uyusur et al.[27] examined the influence of solution chemistry (IS and the presence of surfactant) and the impact of air−liquid and solid−liquid interfaces on the mobility of a CdSe QD in columns packed with sand. These researchers concluded that the mobility of the CdSe QD under unsaturated conditions is mainly controlled by capillary forces. Uyusur et al.[27] suggested that QDs may be highly mobile in dynamic and heterogeneous natural subsurface environments. We also noted in a previous study[25] that the retention of a commercial CdTe QD on a model sand surface was very low at neutral pH.

The few studies aimed at investigating the transport behavior of QDs in granular environments have utilized quartz (clean or coated) as the collector surface of interest.[25−27] There is one study in the literature reporting on the mobility of QDs in soil;[28] however, our understanding of ENP transport potential in this more complex medium is limited. The composition of soil (e.g., mineral content and organic matter content) can differ considerably from one location to another and different ENPs will likely exhibit varying affinity for different soil fractions.[17] This inherent geographical and constitutional heterogeneity of natural soils presents considerable challenges to the development of functional relationships linking ENP physicochemical properties and their transport potential. Nevertheless, well-controlled laboratory studies are needed to identify potential links between measurable ENP and soil properties and the mobility of ENPs in saturated granular environments.

The purpose of this work is to systematically evaluate and compare the transport potential of two carboxyl-terminated commercial QDs and a model nanosized carboxylated polystyrene latex (*n*PL) particle in the following water-saturated granular environments: (i) a clean quartz sand commonly used in ENP transport studies and (ii) loamy sand obtained from a farm near Québec City, QC, Canada. Well-controlled laboratory-scale packed column experiments are performed to study the mobility of the three ENPs in the different granular media over a broad range of environmentally relevant solution IS, examining the influence of both monovalent ($K^+$) and divalent cations ($Ca^{2+}$). This study provides a starting point for the comparison of the transport behavior of ENPs in pure quartz sand versus soil matrices (loamy sand), where greater retention may be observed.

## MATERIALS AND METHODS

**Nanoparticle Suspensions.** Two types of carboxyl-terminated QDs − a CdTe/CdS QD (Vive Nano, Catalog No. 18010 L, stabilized by a poly acrylic acid derivative and suspended in water) and a CdSe/ZnS QD (Ocean Nanotechnologies, Catalog No. QSH530-04, coated with a monolayer of octadecylamine and a monolayer of undisclosed amphiphilic polymer and suspended in water) − with reported nominal sizes of 10 and 14 nm, respectively, were used in this study. In addition, carboxylated *n*PL (24 nm nominal size, Invitrogen, Catalog No. F8787) was used as a model ENP. ENP suspensions were prepared by diluting stock samples in electrolyte of varying IS (1−100 mM KCl or 1−10 mM $CaCl_2$) in deionized water (Biolab) at an adjusted pH of 7 (using HCl or KOH). The nanoparticle suspensions (at concentrations of $10^{12}$ particles/mL for the CdTe QD and *n*PL and $5 \times 10^{12}$ particles/mL for the CdSe QD) were vortexed at high speed for 30 s and then left for 2 h at 9 °C and finally at room temperature for 30 min prior to each experiment.

**Nanoparticle Characterization.** The electrophoretic mobility (EPM) of the ENPs was assessed using a Zetasizer Nano ZS (Malvern Instruments, UK). Each measurement was performed in triplicate using disposable capillary cells with an adjusted electrical field ($E$) between 5 and 10 ± 0.1 V/m. To adequately characterize ENPs in aqueous suspension, we reported in a previous study the necessity of using complementary characterization techniques.[29] Accordingly, the hydrodynamic diameter of the particles was obtained by dynamic light scattering (DLS) (ZetaSizer Nano, Malvern), and under selected conditions the particle size was assessed by transmission electron microscopy (TEM). For DLS, nanoparticle suspensions were prepared in an electrolyte solution (either KCl or $CaCl_2$), and sizing measurements were repeated with at least three different samples. TEM specimens were prepared following the procedure recommended by Mavrocordatos et al.[30] A small droplet (20 μL) of the nanoparticle suspension was placed onto a Formvar carbon-sputtered copper grid (SPI Supplies) followed by air drying overnight prior to analysis. Images were captured with a Philips CM200 TEM equipped with a 2k × 2k CCD camera (Advanced Microscopy Techniques Corp., MA, USA) operating at 200 kV. The mean sizes of the ENPs were determined from the analysis of at least 40 particles per frame, in at least three randomly selected images recorded at high magnification.

**Column Transport Experiments.** ENP transport experiments were conducted using glass chromatography columns (10/20, Amersham Biosciences, Piscataway, NJ) with a 1 cm internal diameter and packed with either quartz sand or loamy sand to a packed bed depth of 10 ± 0.5 cm. Details regarding the porous media characteristics are provided in the Supporting Information (Table S1 and Figure S1). In the case of the quartz sand columns, 13.5 g of dry sand was soaked overnight in electrolyte and then packed into the column and equilibrated with 10 pore volumes (PVs) of the background electrolyte at a constant approach velocity of $1.06 \times 10^{-4}$ m/s (equivalent to a flow rate of 0.5 mL/min). In the case of the loamy sand columns, the packed bed was prepared as described by Jaisi and Elimelech.[31] The dry packing of 11.84 g of loamy sand into the glass column was performed using gentle vibration. The packed column was purged with $CO_2$ in an upward flow direction for 20 min to improve water saturation as suggested by Kretzchmar et al.[32] Next, a solution of 20 mM $CaCl_2$ was injected into the column for 25 PVs, and finally, 100 PVs of the electrolyte of interest were injected into the column (downward flow direction) at an approach velocity of $1.06 \times 10^{-4}$ m/s prior to injection of the ENP suspensions.

In both series of column experiments, 12.5 mL of each ENP suspension (equivalent to 3.7 or 3.3 PVs for quartz sand and loamy sand columns, respectively) were injected into the packed column, and the effluent ENP concentration ($C$) was monitored in real-time with a spectrofluorometer (Fluoromax-4, Jobin-Yvon Horiba) equipped with a flow-through cell. The EX/EM settings for the different ENPs were as follows: 350/538 for the CdTe QD, 350/550 for the CdSe QD, and 505/550 for the *n*PL. The concentration of the influent ENP suspensions ($C_0$) was the same as that used for ENP characterization. ENP transport experiments were conducted over a wide range of solution IS, using both monovalent and

Table 1. Summary of the Electrophoretic Mobility and Particle Size of the ENPs Used in This Study As a Function of Solution IS in KCl or $CaCl_2$ at pH 7

| electrolyte | ionic strength (mM) | particle | electrophoretic mobility ($\mu$m·cm/V·s) | DLS diameter (nm) | TEM diameter (nm) |
|---|---|---|---|---|---|
| KCl | 0.1 | CdTe QD | −2.1 ± 0.5 | 72 ± 1 | 5 ± 2 |
| | 1 | | −2.3 ± 0.4 | 71 ± 1 | |
| | 3 | | −2.2 ± 0.2 | 78 ± 14 | |
| | 10 | | −2.1 ± 0.1 | 83 ± 5 | |
| | 30 | | −1.9 ± 0.7 | 68 ± 12 | |
| | 100 | | −2.0 ± 0.2 | 114 ± 11 | 9 ± 4 |
| KCl | 0.1 | CdSe QD | −1.9 ± 0.4 | 76 ± 28 | 5 ± 2 |
| | 1 | | −2.5 ± 0.2 | 144 ± 62 | |
| | 10 | | −1.0 ± 0.5 | 194 ± 24 | |
| | 100 | | −0.4 ± 0.1 | 175 ± 54 | 42 ± 24 |
| KCl | 0.1 | *n*PL | −4.5 ± 0.2 | 59 ± 1 | |
| | 1 | | −3.9 ± 0.3 | 60 ± 1 | |
| | 3 | | −4.2 ± 0.2 | 69 ± 4 | |
| | 10 | | −3.3 ± 0.3 | 67 ± 2 | |
| | 30 | | −2.9 ± 0.7 | 75 ± 2 | |
| | 100 | | −1.7 ± 0.3 | 86 ± 5 | |
| $CaCl_2$ | 0.1 | CdTe QD | −2.4 ± 0.5 | 59 ± 2 | |
| | 1 | | −1.5 ± 0.2 | 59 ± 1 | |
| | 2.5 | | −1.8 ± 0.1 | 139 ± 3 | |
| | 5 | | −1.9 ± 0.0 | 593 ± 35 | |
| | 10 | | −0.2 ± 0.1 | 447 ± 351 | |
| $CaCl_2$ | 0.1 | CdSe QD | −1.4 ± 0.3 | 257 ± 67 | |
| | 1 | | −1.2 ± 0.1 | 208 ± 4 | |
| | 2.5 | | −1.3 ± 0.0 | 551 ± 58 | 74 ± 30 |
| | 10 | | −0.2 ± 0.1 | 674 ± 146 | |
| $CaCl_2$ | 0.1 | *n*PL | −1.4 ± 0.2 | 97 ± 1 | |
| | 1 | | −1.2 ± 0.2 | 91 ± 4 | |
| | 2.5 | | −1.2 ± 0.2 | 201 ± 318 | |
| | 5 | | −1.5 ± 0.1 | 515 ± 142 | |
| | 10 | | −1.5 ± 0.0 | 2355 ± 816 | |

divalent background electrolyte solutions. Each column experiment was conducted at least twice, and the breakthrough behavior of an inert tracer − the fluorescent dye sodium naphtionate (Fluka Chemika) − was verified prior to injecting the ENP suspensions.

**Interpretation of ENP Transport Experiments.** To quantitatively compare the ENP transport behavior under different experimental conditions, the particle attachment efficiency ($\alpha$) was calculated using colloid filtration theory (CFT), as follows[33]

$$\alpha = -\frac{2}{3}\frac{d_{50}}{(1\text{-}\varepsilon)L\eta_0}\ln\left(\frac{C}{C_0}\right) \quad (1)$$

where $d_{50}$ is the average diameter of the sand grains, $\varepsilon$ is the bed porosity, and $L$ is the packed-bed length. The value of $C/C_0$ in eq 1 represents the normalized column effluent particle concentration for each experiment which was evaluated by numerical integration of the breakthrough curves. Values of $\eta_0$ for each experimental condition were determined using the correlation developed by Tufenkji and Elimelech.[33]

## RESULTS AND DISCUSSION

**Electrophoretic Mobility (EPM) of the ENPs.** The EPM of the three studied ENPs was assessed prior to each transport experiment in the presence of monovalent (KCl) and divalent ($CaCl_2$) salts (Table 1). The three ENPs are negatively charged under the conditions used in this study (pH 7, range of solution IS). The negative surface potential is attributed to the presence of carboxyl groups in the surface coatings of the ENPs.

In general, when the ENPs are suspended in the monovalent salt KCl, they become less negative as the IS increases due to compression of the electrical double layer (Table 1). Although this decrease in the absolute EPM is quite dramatic for the *n*PL and CdSe QD when the salt concentration is increased from 0.1 to 100 mM KCl, the effect is not as significant for the CdTe QD (EPM changes only from −2.1 to −2.0 $\mu$m·cm/V·s). The variation in EPM with IS for the *n*PL is consistent with soft particle theory; namely, the EPM becomes less negative with increasing IS but stabilizes at a nonzero value.[34,35] The EPM of the poly acrylic acid (PAA) coated CdTe QD also stabilizes at a nonzero value but barely changes over the wide range of IS. At low IS, the *n*PL is significantly more negative than the QDs (EPM = −4.5 $\mu$m·cm/V·s, whereas the EPM for the CdSe QD and the CdTe QD is on the order of −1.9 and −2.1 $\mu$m·cm/V·s, respectively). This result is consistent with the information


dx.doi.org/10.1021/es2045458 | Environ. Sci. Technol. 2012, 46, 4449−4457

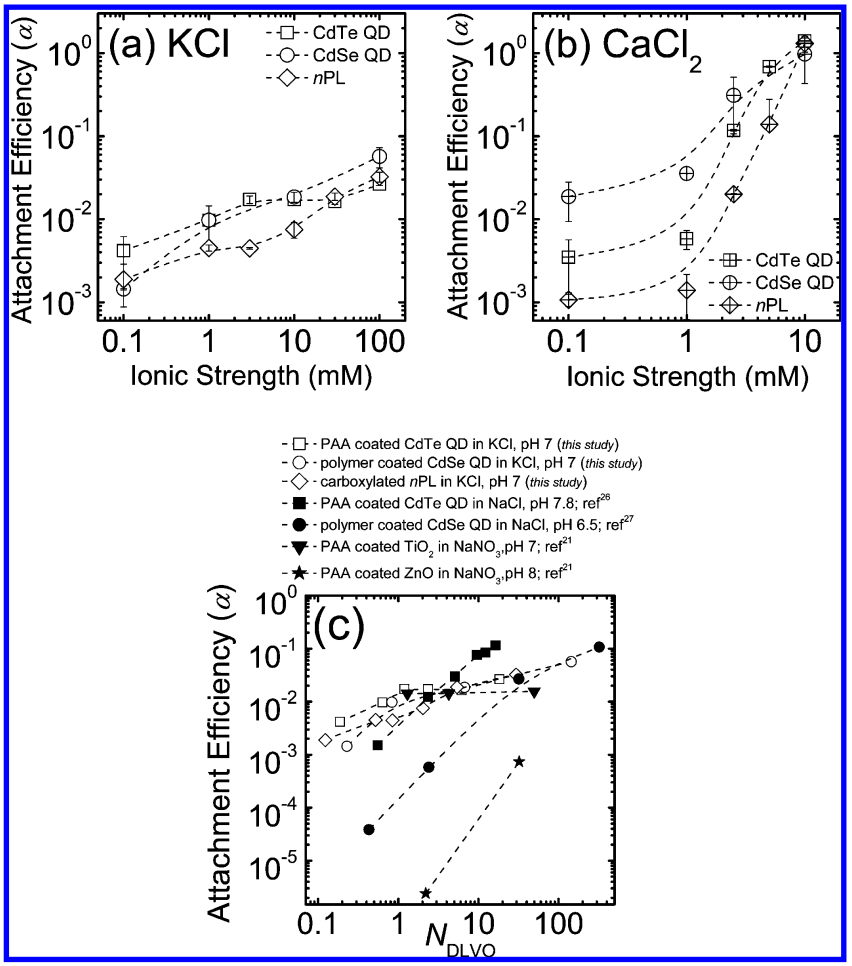


**Figure 1.** Attachment efficiencies ($\alpha$) calculated using eq 1 for the (□) CdTe QDs, (○) CdSe QDs, and (◊) *n*PL particles suspended in electrolyte over a wide range of solution ionic strengths (pH 7). Experiments were conducted using columns packed with clean quartz sand, and particles were suspended in (a) KCl or (b) $CaCl_2$. Dashed lines are included as eye guides, and error bars represent 95% confidence intervals. (c) Calculated ENP attachment efficiencies ($\alpha$) evaluated for different ENPs in columns packed with quartz sand plotted as a function of the dimensionless parameter $N_{DLVO}$. Attachment efficiencies were calculated using eq 1 and the correlation developed by Tufenkji and Elimelech.[33] Open symbols represent the ENPs used in the present study, and solid symbols represent experimental data adapted from other studies.[21,26,27].

provided by the ENP vendors: the amount of carboxylate groups on the *n*PL is on the order of $3 \times 10^3$ per particle (Invitrogen), $1.2 \times 10^2$ for each CdSe QD (Ocean Nano), and a similar order of magnitude for the CdTe QD (although specific details were undisclosed by Vive Nano).

The *n*PL is significantly less negative when suspended in $CaCl_2$, and the EPM is stable over the range of IS examined (Table 1). The variation in the measured EPM over the range of IS is much more important for the two QDs. The EPM changes from −2.4 to −0.2 $\mu$m·cm/V·s for the CdTe QD and from −1.4 to −0.2 $\mu$m·cm/V·s for the CdSe QD when the IS increases from 0.1 to 10 mM $CaCl_2$. Both QDs nearly reach their point of zero charge (PZC) at an IS of 10 mM $CaCl_2$.

These EPM measurements are in general agreement with other published studies examining functionalized QDs.[26,27,36] When converted to zeta potentials using the Henry equation[37] and the expression for the retardation effect of "hard spherical" particles proposed by Ohshima[38] (Table S2), our results are comparable to those reported by Torkzaban et al.[26] for a carboxylated CdTe QD. These researchers reported zeta potentials on the order of −45 to −35 mV in NaCl (pH 7.8), and Zhang et al. reported values between −30 to −20 mV in KCl (pH 7)[36] for a thioglycolate functionalized CdTe QD in a range of IS from 1 to 100 mM. Likewise, Uyusur et al.[27] reported values of −41 and 0 mV for a polymer coated (octylamine with modified poly acrylic-acid) CdSe QD in 0.5 mM and 500 mM NaCl (pH 6.5), respectively. As indicated above, the ENPs studied here each have different surface coatings, but for each ENP, the terminal functional group is carboxylate.

**Size Analysis of the ENPs.** Nanoparticle size is an important parameter in the interpretation of nanoparticle transport and fate studies in granular aquatic environments.[18] However, sizing suspended ENPs can be challenging given the limitations of available experimental techniques.[29]

DLS enables rapid analysis and is one of the most widely used methods of assessing particle size in aqueous samples. DLS measurements of the QD suspensions used in this study are presented based on intensity based distributions (z-average) and generally exhibit an overall increase in hydrodynamic diameter ($d_h$) with increasing KCl or $CaCl_2$ concentration (Table 1). The hydrodynamic diameter increases from 72 to 114 nm for the CdTe QD, between 76 to 175 nm for the CdSe QD, and from 59 to 86 nm for the model particle *n*PL over the studied range of IS (0.1 to 100 mM) in monovalent salt solution. All of the particles exhibit significant aggregation when


dx.doi.org/10.1021/es2045458 | Environ. Sci. Technol. 2012, 46, 4449–4457

suspended in a divalent salt solution at the studied range of IS (0.1 to 10 mM $CaCl_2$). At an IS of 2.5 mM $CaCl_2$, the $d_h$ increases significantly for all three ENPs (from 59 to 139 nm for CdTe QD, from 208 to 551 nm for CdSe QD and from 91 to 201 nm for *n*PL) (Table 1). The marked aggregation behavior for carboxylated QDs in the presence of multivalent cations (e.g., $Mg^{2+}$ or $Ca^{2+}$) has been previously reported by Zhang et al.[36]

The use of DLS has been criticized because the scattering intensity varies strongly with the particle diameter (i.e., to the sixth power), which biases the interpretation of particle size ($d_h$) toward larger particles. Hence, DLS should not be employed as the sole characterization method. As a complementary characterization tool, TEM was employed to image the QDs under selected conditions. Although the use of TEM is not ideal due to the drying procedure used to prepare samples for imaging,[29] this technique can be useful for evaluating the extent of aggregation of nanoparticle suspensions. The samples analyzed by TEM were prepared in the same manner as those used for the column experiments, with an additional step needed for sample drying. At low IS (0.1 mM KCl, pH 7), the studied nanoparticles are generally well dispersed in the aqueous medium, and large aggregates are not observed (Figure S2a, b, d, e). Using the image analysis software Image J, the nominal particle sizes were determined by measuring individual particles in a series of TEM images (Table 1). At this low IS (0.1 mM KCl), the QDs are slightly smaller than the nominal particle size reported by the manufacturer (on the order of 5 ± 2 nm for the CdTe QD and 9 ± 4 nm for the CdSe QD). When the IS is increased to 100 mM KCl, the nominal size of the CdTe QD is on the same order of magnitude (9 ± 4 nm), while the CdSe QD experienced some aggregation (42 ± 24 nm). In the presence of 2 mM IS $CaCl_2$, the aggregation is more significant for both QDs (Figure S2c and f). The particles in Figure S2f seem to be adhered to one another as opposed to forming aggregates. This may be an artifact of the sample preparation procedure or a result of particle dissolution. However, measurements of changes in the free $[Cd^{2+}]$ during the time scale of the column experiments reveal little dissolution of both types of QDs at the experimental conditions of this study (on the order of 0.3% in KCl and on the order of 2% in $CaCl_2$) (Table S3).

## NANOPARTICLE TRANSPORT IN QUARTZ SAND AND LOAMY SAND

**Transport and Deposition of Three ENPs in Saturated Quartz Sand.** Figure S3 shows representative particle breakthrough curves for experiments conducted with the 3 ENPs suspended in KCl solution where the normalized particle concentration at the column effluent ($C/C_0$) is plotted as a function of PVs (dimensionless time). The data show that an increase in concentration of KCl does not have a major influence on the breakthrough QD concentration at the column effluent. Although we generally observe increased retention of QDs with increasing salt concentration, the effect is not dramatic. Overall, the three ENPs are highly mobile in the quartz sand in the presence of a monovalent salt (KCl). Numerical integration of the area under each breakthrough curve reveals that only 24% of the CdTe QDs are retained in the packed sand column at the highest IS examined (Table S2). Likewise, only 17% and 33% of the CdSe QD and *n*PL particles, respectively, are retained in the experiments conducted at 100 mM KCl. In the case of the model particle (*n*PL), the breakthrough curves at higher salt concentrations (above 10 mM) show the distinctive shape characteristic of "blocking".[39,40] Under certain conditions, particles deposited on the collector (sand grain) surface can "block" the deposition of suspended particles, resulting in a characteristic elution profile with rapidly increasing particle concentration with time.[39]

Figure 1 summarizes the calculated $\alpha$ values for the three ENPs when suspended in the monovalent electrolyte (KCl, Figure 1a) or the divalent electrolyte ($CaCl_2$, Figure 1b). In KCl, the nanoparticle attachment efficiency is relatively low (below 0.1) over the entire range of IS examined. The calculated $\alpha$ values increase with IS (e.g., from 0.004 to 0.026 for the CdTe QD; 0.001 to 0.057 for the CdSe QD; and from 0.002 to 0.032 for *n*PL); however, $\alpha$ does not reach the theoretical mass-transfer limited maximum value of unity even at 100 mM KCl. The ENP characterization data presented previously (Table 1) shows that the EPM (or surface potential) generally becomes less negative with increasing salt concentration. Hence, for each individual ENP, the particle attachment behavior observed in the presence of a monovalent electrolyte is generally in qualitative agreement with the DLVO theory of colloidal stability whereby the extent of physicochemical attachment increases with decreasing absolute surface potential.[41,42]

Other studies examining the transport and deposition of polymer-coated QDs have also reported relatively low particle deposition rates on sand or model silica surfaces.[25−27] Using laboratory-scale packed column experiments, Torkzaban et al.[26] showed that the deposition of a CdTe QD was low at salt concentrations up to 100 mM NaCl (buffered to pH 7.8 with $NaHCO_3$). Likewise, Uyusur et al.[27] reported 9% and 4% retention of a CdSe QD in columns packed with quartz sand when the nanoparticles were suspended in 5 and 50 mM NaCl, respectively. Using a quartz crystal microbalance,[25] we previously reported that the deposition of a different carboxylated CdTe QD onto silica is negligible even at high IS (>100 mM KCl, pH 7). We have also observed[20] low $\alpha$ values ($0.01 < \alpha < 0.2$) for deposition of 50 nm sulfate-functionalized *n*PL onto quartz sand over a wide range of KCl concentrations (1−100 mM KCl) at pH 5.5. Hence, the results we report here are in qualitative agreement with other studies of QD and *n*PL deposition on quartz.

Figure 1b shows the attachment efficiencies of the three ENPs when suspended in the divalent electrolyte ($CaCl_2$) at pH 7. A more significant change in $\alpha$ is noted as the IS of $CaCl_2$ increases from 0.1 to 10 mM (versus that observed for the monovalent salt), and for all three ENPs, $\alpha$ reaches the theoretical maximum (~1) at the highest IS. Also, above 1 mM IS, the ENP deposition rates are greater in $CaCl_2$ than in KCl. This observation is attributable to the ability of divalent cations (such as $Ca^{2+}$) to screen particle charge but also to complex with negatively charged groups on the ENP surfaces, effectively decreasing the surface potential and the stability of the particle suspension (see Table 1).[36]

Overall, the data reported here for the transport of the two different QDs in quartz sand points to a mechanism of electrosteric stabilization resulting from the presence of the polymer and polyelectrolyte coatings on the ENP surfaces.[22,43,44] Namely, we observe relatively low retention of the QDs over a very broad range of KCl concentrations. This stabilization effect is less apparent at high concentrations of the divalent salt $CaCl_2$, likely due to charge screening and compression of the macromolecules on the particle surfaces.

Interestingly, comparable low extents of deposition are observed with the unmodified *n*PL particle, although such particles are generally not considered to be electrosterically stabilized. The limited retention of the *n*PL particle in the presence of the monovalent electrolyte is likely governed by electrostatic stabilization due to its significant surface potential (Table 1).

As mentioned above, there are limited studies examining the transport and deposition of QDs in saturated granular systems. Figure 1c presents a comparison of data from column transport studies conducted with QDs and selected other surface-modified nanomaterials in different laboratories.[21,26,27] Data included in Figure 1c include those for experiments in saturated quartz sand with a CdTe QD[26] and CdSe QD[27] as well as metal oxide nanoparticles ($n$TiO$_2$ and $n$ZnO)[21] coated with the same PAA derivative as that used for the CdTe QD used in this study. In this figure, the particle attachment efficiency is plotted as a function of the dimensionless parameter $N_{DLVO}$,[45] which takes into account the key experimental conditions used in each study (eq 2)

$$N_{DLVO} = \frac{\kappa A}{\varepsilon_0 \varepsilon_r \psi_c \psi_p} \quad (2)$$

Here, $\kappa$ is the inverse Debye length, $A$ is the Hamaker constant for the ENP-water-collector systems[18] used in each study, $\psi_c$ is the surface (zeta) potential for the collector surface, $\psi_p$ is the surface (zeta) potential for each ENP, $\varepsilon_0$ is the dielectric permittivity in vacuum, and $\varepsilon_r$ is the relative dielectric permittivity of water. It should be noted that the dimensionless parameter $N_{DLVO}$ does not consider the potential steric contributions of the particle surface coatings which may vary for the different ENPs examined.

Inspection of Figure 1c reveals that all of the studied ENPs (with the exception of $n$TiO$_2$) exhibit decreased mobility with increasing values of $N_{DLVO}$ in water-saturated quartz sand. In many cases, the values of $\alpha$ fall within the same region of the plot (except for the CdSe QD data from ref 27 and for the $n$ZnO data from ref 21). Values of the attachment efficiency determined from the data reported by Torkzaban et al.[26] (for the same CdTe QD as that used in this study) are comparable to our results at moderate IS ($N_{DLVO} < 5$) but approximately 1 order of magnitude larger at the highest IS examined ($N_{DLVO} \approx 20$). Conversely, the results reported by Uyusur et al.[27] for a polymer-coated CdSe QD (under saturated conditions) result in lower $\alpha$ values than those measured here within a large range of solution IS ($0.5 < N_{DLVO} < 300$). Likewise, Petosa et al.[21] reported very low retention for a PAA-coated ZnO nanoparticle when $N_{DLVO} < 20$. The significant mobility of the ZnO nanoparticle is surprising given that it is prepared by the same manufacturer and with the same polymeric coating as the CdTe QD used in this study (open squares in Figure 1c). The transport behavior of the ZnO nanoparticle was examined in the same quartz sand used in the present study.[21] However, the hydrodynamic diameter of the ZnO particles (measured by DLS) was significantly lower (on the order of 10 nm at 10−100 mM NaNO$_3$) than the size of the CdTe QD used in this study (on the order of 114 nm at 100 mM KCl). In all the cases reported in Figure 1c, the maximum $\alpha$ value for ENP deposition onto quartz sand is far from the theoretical maximum ($\alpha = 1$) even at high $N_{DLVO}$ values. Thus, the limited data available to date on the mobility of QDs suggest that the transport potential of this ENP in water-saturated quartz sand can be significant in the absence (or at low concentrations) of divalent salts.

**Transport and Deposition of QDs and *n*PL in Loamy Sand.** An additional series of ENP transport experiments was carried out using columns packed with loamy sand obtained from a farm in St-Augustin-de-Desmaures, QC. Although the loamy sand columns were not extracted as undisturbed cores, the comparison of ENP transport and deposition in quartz sand to loamy sand is useful for evaluating the influence of collector grain properties on the filtration process. The collector media differ with respect to surface chemistry, grain size distribution, and geochemical heterogeneity.

The grain size distributions of the quartz and loamy sand obtained by sieve analysis are shown in Figure S1. The mean grain size ($d_{50}$) of the two granular materials is comparable (0.256 mm for the quartz sand versus 0.225 mm for the loamy sand); however, the size distribution of the quartz sand is more uniform (coefficient of uniformity, $d_{60}/d_{10} = 1.4$) than that of the loamy sand ($d_{60}/d_{10} = 2.1$).

Figure 2 illustrates representative BTCs for transport experiments conducted with the three ENPs using columns packed with the loamy sand over a wide range of solution IS

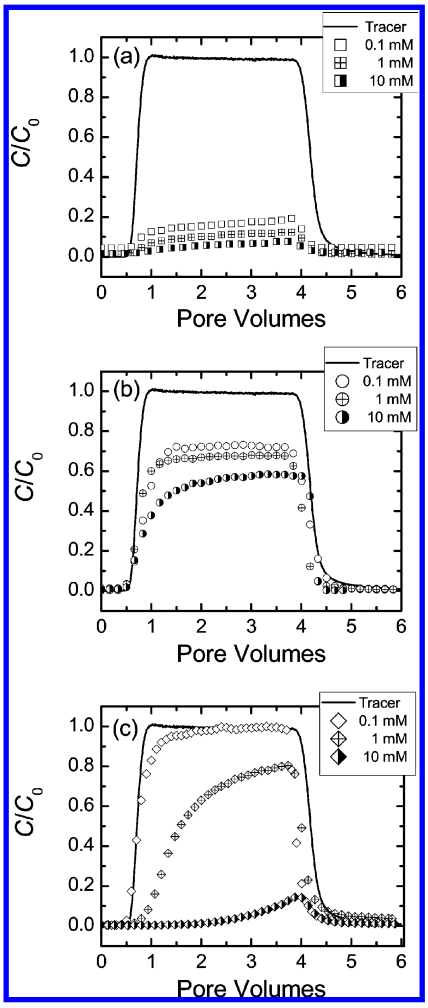


**Figure 2.** Representative breakthrough curves for (a) CdTe QDs, (b) CdSe QDs, and (c) *n*PL in columns packed with loamy sand at selected KCl concentrations. The breakthrough behavior of a conservative fluorescent tracer (sodium naphthionate) is also shown (solid line).

(0.1−10 mM KCl). As the concentration of KCl increases, the extent of particle retention increases for all three ENPs. However, it is interesting to note that the rate of change in the nanoparticle deposition rate with respect to IS is quite different for each ENP. For example, ∼80% of the CdTe QDs are retained in the loamy sand column at 0.1 mM IS (Figure 2a), and the extent of retention increases to 90% at 10 mM. The retention of the CdSe QD (Figure 2b) ranges from 29% to 43% in the same range of IS. In contrast, the *n*PL particle exhibits a faster change in the particle deposition rate with IS; namely, the extent of retention increases from 5% to 93% when the IS is changed from 0.1 to 10 mM (Figure 2c). As noted above for the experiments conducted with columns packed with quartz sand (Figure S2c), inspection of Figure 2c reveals that the BTCs for the *n*PL particle again exhibit the characteristic "blocking" profile at 1 and 10 mM IS.[39,46] At the lower IS examined (0.1 mM), the effluent *n*PL particle concentration stabilizes at approximately 2 PVs; hence, the breakthrough curve is generally flat after this time point. For the higher IS displayed in Figure 2c, the breakthrough concentrations of the *n*PL particle do not reach a steady value but rather continue to increase with time. This observed increase in effluent particle concentration with time is attributed to the reduced availability of deposition sites on the collector grains as deposited particles exclude the local surrounding collector surface area from deposition of incoming particles.[40]

For the sake of quantitatively comparing the results obtained from the loamy sand packed columns with the data from the quartz sand experiments (Figure S3 and Table S2), ENP attachment efficiencies were evaluated from each BTC and are presented in Figure 3. For the PAA-coated CdTe QD, $\alpha$ values

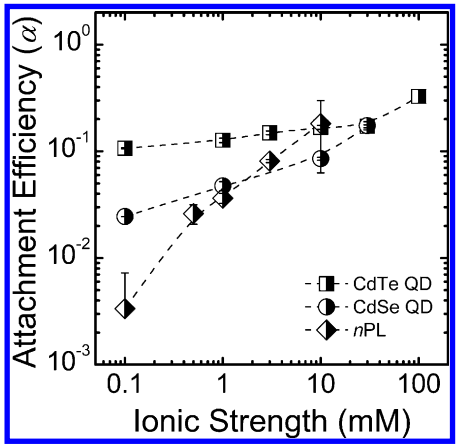


**Figure 3.** Calculated attachment efficiencies ($\alpha$) for the three ENPs in loamy sand suspended in KCl at pH 7. The experimental conditions are as follows: approach velocity ($U$) 1.06 × $10^{-4}$ m/s, porosity ($\varepsilon$) 0.47, mean grain diameter ($d_{50}$) 0.225 mm, and temperature 20−22 °C. Error bars represent 95% confidence intervals.

are approximately an order of magnitude greater in the loamy sand (Figure 3) when compared to the quartz sand (Figure 1a). The CdSe QD also exhibits higher $\alpha$ values in the loamy sand matrix, but the extent of retention is generally lower than that measured for the CdTe QD. In these loamy sand column experiments, the *n*PL particle exhibits the greatest change in $\alpha$ with increasing IS; namely, $\alpha$ increases from 0.003 to 0.18 when the salt concentration increases from 0.1 to 10 mM KCl. The *n*PL particle is also considerably less mobile in the loamy sand than in the quartz sand.

This is the first study comparing the transport behavior of QDs in quartz sand and loamy sand in water-saturated conditions. The loamy sand characterized by nitrogen BET adsorption isotherms has considerably larger surface area and porosity than the quartz sand (Table S1). Characterization of the loamy sand indicates that it is mainly composed of quartz (88.2%), but it also contains clay-sized particles (7.6%) and organic matter (0.44%). EDS analysis reveals the heterogeneous composition of the loamy sand (mainly Si, Al, Fe) is in qualitative agreement with the mineralogical composition of the medium: silicon dioxide, feldspars (albite and orthoclase), and amorphous clay (allophane). The mineralogy of the granular collectors and the solution chemistry of the pore fluid will affect the mechanisms of ENP retention. For instance, allophane (present in the clay fraction) can present positively charged sites (PZC∼7.8) where negatively charged ENPs can "favorably" deposit, whereas albite (PZC∼5.9) and orthoclase (PZC∼1) present unfavorable conditions for retention of these ENPs.[47]

This study was conducted at neutral pH; however, natural variations in pore water pH are expected to affect the fate of QDs in natural subsurface environments.[17,25,36] Zhang et al.[36] reported on the stability of a polymer coated CdTe QD in monovalent electrolyte at different pHs. Good colloidal stability (i.e., no aggregation) was observed at pHs between 5 and 12, due to electrostatic repulsion exerted by the anionic polymer coating. At lower pHs (3 and 2), these researchers observed the presence of important QD instability with the formation of aggregates on the order of a few micrometers in size. Navarro et al.[17] investigated the effect of pH on the interaction between a CdSe QD and humic substances. Here, the interaction between the humics and the QD was greatly enhanced under acidic conditions (pH 3), compared with more alkaline conditions (pH 7 and pH 9). In an earlier study,[25] we also reported the effect of pH on the deposition behavior of a CdTe QD onto a model sand surface; namely, the deposition rate of the CdTe QD was higher at lower pH (5 versus 7). Because pH influences critical particle and collector surface and physical properties (e.g., particle aggregate size, particle surface potential, collector surface potential, etc.), future studies should be aimed at clarifying the role that pH plays in QD transport and deposition in natural soil systems.

**Environmental Implications.** A myriad of new ENPs are being introduced onto the commercial market each year, yet the environmental fate and potential risks linked with these materials are not properly understood. Moreover, the variability in the composition of the core and surface coatings of commercial ENPs renders predictions of their transport potential and associated contamination risks very challenging. Well-controlled laboratory column experiments conducted with two representative QDs show that these nanoparticles can exhibit quite similar deposition behavior onto a clean quartz sand collector over a broad range of solution conditions (Figure 1). Furthermore, the selected *n*PL particle appears to be a good model material for determining conservative estimates of the transport potential of these two QDs in the quartz sand matrix. However, the transport potential of the two QDs is different in the loamy sand system, whereby the CdTe QD exhibits greater retention than the CdSe QD (Figure 3). This divergence in the transport behavior of the two QDs in the loamy sand matrix is likely linked to differences in the chemistry of the polymeric coatings on the ENP surfaces. The chemical composition of polymers used to functionalize ENP surfaces will influence the

polymer affinity (and hence ENP affinity) for clay surfaces.[23,26] For instance, Zaman et al.[48] found a strong bridging interaction between PAA molecules and alumina-like charged sites on the edges of clay particles. The nature of the coating molecules on ENP surfaces will also control the potential for degradation of the coatings and the likelihood for ligand exchange, which will influence the aqueous dispersibility, mobility and stability of the particles in aquatic subsurface environments.[28] Because of the common practice of using polymeric coatings for stabilization of ENPs, additional studies aimed at understanding the role of such coatings in ENP transport, aggregation, and environmental fate is of particular importance.

The inherent heterogeneity of natural granular materials found in subsurface environments remains another major challenge for the development of functional relationships between soil properties and ENP transport potential. Although the two granular matrices used in this study have comparable mean grain diameters, the retention of the 3 ENPs is generally higher in the loamy sand versus the quartz sand. Thus, further research is needed to extend this work to a wider range of environmentally relevant granular matrices and water chemistries.

## ■ ASSOCIATED CONTENT

### Supporting Information

Details on granular media preparation and characterization, QD dissolution behavior, QD characterization by TEM, and additional representative ENP breakthrough curves with summarized data from column experiments. This material is available free of charge via the Internet at http://pubs.acs.org.

## ■ AUTHOR INFORMATION

### Corresponding Author

*Phone: (514) 398-2999. Fax: (514) 398-6678. E-mail: nathalie.tufenkji@mcgill.ca.

### Notes

The authors declare no competing financial interest.

## ■ ACKNOWLEDGMENTS

The authors acknowledge the financial support of the Natural Sciences and Engineering Research Council of Canada (NSERC), Le Fonds québécois de la recherche sur la nature et les technologies (FQRNT), Environment Canada, Vive Nano, the McGill Engineering Doctoral Award (MEDA) Program, the Eugenie Ulmer Lamothe (EUL) fund at McGill and CONACYT-Mexico.

## ■ REFERENCES

(1) Roco, M.; Mirkin, C.; Hersam, M. Nanotechnology research directions for societal needs in 2020: summary of international study. *J. Nanopart. Res.* **2011**, *13* (3), 897−919.

(2) Auffan, M.; Rose, J.; Bottero, J.-Y.; Lowry, G. V.; Jolivet, J.-P.; Wiesner, M. R. Towards a definition of inorganic nanoparticles from an environmental, health and safety perspective. *Nat. Nanotechnol.* **2009**, *4* (10), 634−641.

(3) Baalousha, M.; Lead, J. R. Overview of Nanoscience in the Environment. In *Environmental and Human Health Impacts of Nanotechnology*; John Wiley & Sons, Ltd.: 2009; pp 1−29.

(4) Bruchez, M. Jr.; Moronne, M.; Gin, P.; Weiss, S.; Alivisatos, A. P. Semiconductor nanocrystals as fluorescent biological labels. *Science* **1998**, *281* (5385), 2013−2016.

(5) Murray, C. B.; Norris, D. J.; Bawendi, M. G. Synthesis and characterization of nearly monodisperse CdE (E = S, Se, Te) semiconductor nanocrystallites. *J. Am. Chem. Soc.* **1993**, *115* (19), 8706−8715.

(6) Alivisatos, A. P. The use of nanocrystals in biological detection. *Nat. Biotechnol.* **2004**, *22* (1), 47−52.

(7) Nozik, A. J. Quantum dot solar cells. *Physica E* **2002**, *14* (1−2), 115−120.

(8) Posani, K. T.; Tripathi, V.; Annamalai, S.; Weisse-Bernstein, N. R.; Krishna, S.; Perahia, R.; Crisafulli, O.; Painter, O. J. Nanoscale quantum dot infrared sensors with photonic crystal cavity. *Appl. Phys. Lett.* **2006**, *88*, 15.

(9) Dabbousi, B. O.; Rodriguez-Viejo, J.; Mikulec, F. V.; Heine, J. R.; Mattoussi, H.; Ober, R.; Jensen, K. F.; Bawendi, M. G. CdSe)ZnS core-shell quantum dots: Synthesis and characterization of a size series of highly luminescent nanocrystallites. *J. Phys. Chem. B* **1997**, *101* (46), 9463−9475.

(10) Clark, R. J.; Dang, M. K. M.; Veinot, J. G. C. Exploration of Organic Acid Chain Length on Water-Soluble Silicon Quantum Dot Surfaces. *Langmuir* **2010**, *26* (19), 15657−15664.

(11) Park, J. H.; Gu, L.; Von Maltzahn, G.; Ruoslahti, E.; Bhatia, S. N.; Sailor, M. J. Biodegradable luminescent porous silicon nanoparticles for in vivo applications. *Nat. Mater.* **2009**, *8* (4), 331−336.

(12) Domingos, R. F.; Simon, D. F.; Hauser, C.; Wilkinson, K. J. Bioaccumulation and Effects of CdTe/CdS Quantum Dots on Chlamydomonas reinhardtii − Nanoparticles or the Free Ions? *Environ. Sci. Technol.* **2011**, *45* (18), 7664−7669.

(13) Hoshino, A.; Fujioka, K.; Oku, T.; Suga, M.; Sasaki, Y. F.; Ohta, T.; Yasuhara, M.; Suzuki, K.; Yamamoto, K. Physicochemical properties and cellular toxicity of nanocrystal quantum dots depend on their surface modification. *Nano Lett.* **2004**, *4* (11), 2163−2169.

(14) Lovric, J.; Bazzi, H. S.; Cuie, Y.; Fortin, G. R. A.; Winnik, F. M.; Maysinger, D. Differences in subcellular distribution and toxicity of green and red emitting CdTe quantum dots. *J. Mol. Med.* **2005**, *83* (5), 377−385.

(15) Darlington, T. K.; Neigh, A. M.; Spencer, M. T.; Nguyen, O. T.; Oldenburg, S. J. Nanoparticle characteristics affecting environmental fate and transport through soil. *Environ. Toxicol. Chem.* **2009**, *28* (6), 1191−1199.

(16) Holbrook, R. D.; Murphy, K. E.; Morrow, J. B.; Cole, K. D. Trophic transfer of nanoparticles in a simplified invertebrate food web. *Nat. Nanotechnol.* **2008**, *3* (6), 352−355.

(17) Navarro, D. A. G.; Watson, D. F.; Aga, D. S.; Banerjee, S. Natural organic matter-mediated phase transfer of quantum dots in the aquatic environment. *Environ. Sci. Technol.* **2009**, *43* (3), 677−682.

(18) Petosa, A. R.; Jaisi, D. P.; Quevedo, I. R.; Elimelech, M.; Tufenkji, N. Aggregation and deposition of engineered nanomaterials in aquatic environments: Role of physicochemical interactions. *Environ. Sci. Technol.* **2010**, *44* (17), 6532−6549.

(19) Fatisson, J.; Ghoshal, S.; Tufenkji, N. Deposition of carboxymethylcellulose-coated zero-valent iron nanoparticles onto silica: Roles of solution chemistry and organic molecules. *Langmuir* **2010**, *26* (15), 12832−12840.

(20) Pelley, A. J.; Tufenkji, N. Effect of particle size and natural organic matter on the migration of nano- and microscale latex particles in saturated porous media. *J. Colloid Interface Sci.* **2008**, *321* (1), 74−83.

(21) Petosa, A. R.; Brennan, S. J.; Rajput, F.; Tufenkji, N. Transport of two metal oxide nanoparticles in saturated granular porous media: Role of water chemistry and particle coating. *Water Res.* **2012**, *46* (4), 1273−1285.

(22) Phenrat, T.; Song, J. E.; Cisneros, C. M.; Schoenfelder, D. P.; Tilton, R. D.; Lowry, G. V. Estimating Attachment of Nano- and Submicrometer-particles Coated with Organic Macromolecules in Porous Media: Development of an Empirical Model. *Environ. Sci. Technol.* **2010**, *44* (12), 4531−4538.

(23) Saleh, N.; Kim, H. J.; Phenrat, T.; Matyjaszewski, K.; Tilton, R. D.; Lowry, G. V. Ionic strength and composition affect the mobility of surface-modified $Fe^0$ nanoparticles in water-saturated sand columns. *Environ. Sci. Technol.* **2008**, *42* (9), 3349−3355.

(24) Sirk, K. M.; Saleh, N. B.; Phenrat, T.; Kim, H.-J.; Dufour, B.; Ok, J.; Golas, P. L.; Matyjaszewski, K.; Lowry, G. V.; Tilton, R. D. Effect of Adsorbed Polyelectrolytes on Nanoscale Zero Valent Iron Particle Attachment to Soil Surface Models. *Environ. Sci. Technol.* **2009**, *43* (10), 3803−3808.
(25) Quevedo, I. R.; Tufenkji, N. Influence of solution chemistry on the deposition and detachment kinetics of a CdTe quantum dot examined using a quartz crystal microbalance. *Environ. Sci. Technol.* **2009**, *43* (9), 3176−3182.
(26) Torkzaban, S.; Kim, Y.; Mulvihill, M.; Wan, J.; Tokunaga, T. K. Transport and deposition of functionalized CdTe nanoparticles in saturated porous media. *J. Contam. Hydrol.* **2010**, *118* (3−4), 208−217.
(27) Uyusur, B.; Darnault, C. J. G.; Snee, P. T.; Kokën, E.; Jacobson, A. R.; Wells, R. R. Coupled effects of solution chemistry and hydrodynamics on the mobility and transport of quantum dot nanomaterials in the vadose zone. *J. Contam. Hydrol.* **2010**, *118* (3−4), 184−198.
(28) Navarro, D. A.; Banerjee, S.; Watson, D. F.; Aga, D. S. Differences in Soil Mobility and Degradability between Water-Dispersible CdSe and CdSe/ZnS Quantum Dots. *Environ. Sci. Technol.* **2011**, *45* (15), 6343−6349.
(29) Domingos, R. F.; Baalousha, M. A.; Ju-Nam, Y.; Reid, M. M.; Tufenkji, N.; Lead, J. R.; Leppard, G. G.; Wilkinson, K. J. Characterizing manufactured nanoparticles in the environment: Multimethod determination of particle sizes. *Environ. Sci. Technol.* **2009**, *43* (19), 7277−7284.
(30) Mavrocordatos;, D.; Perret, D.; Leppard, G. G., Strategies and advances in the characterisation of environmental colloids by electron microscopy. In *Environmental Colloids and Particles: Behaviour, Separation and Characterisation*; Wilkinson, K. J., Lead, J. R., Eds.; John Wiley & Sons: Chichester, UK, 2007; pp 345−404.
(31) Jaisi, D. P.; Elimelech, M. Single-walled carbon nanotubes exhibit limited transport in soil columns. *Environ. Sci. Technol.* **2009**, *43* (24), 9161−9166.
(32) Kretzschmar, R.; Barmettler, K.; Grolimund, D.; Yan, Y. D.; Borkovec, M.; Sticher, H. Experimental determination of colloid deposition rates and collision efficiencies in natural porous media. *Water Resour. Res.* **1997**, *33* (5), 1129−1137.
(33) Tufenkji, N.; Elimelech, M. Correlation Equation for Predicting Single-Collector Efficiency in Physicochemical Filtration in Saturated Porous Media. *Environ. Sci. Technol.* **2004**, *38* (2), 529−536.
(34) Ohshima, H. Electrophoretic Mobility of Soft Particles. *J. Colloid Interface Sci.* **1994**, *163* (2), 474−483.
(35) Ohshima, H. Electrophoresis of soft particles. *Adv. Colloid Interface Sci.* **1995**, *62* (2−3), 189−235.
(36) Zhang, Y.; Chen, Y.; Westerhoff, P.; Crittenden, J. C. Stability and removal of water soluble CdTe quantum dots in water. *Environ. Sci. Technol.* **2008**, *42* (1), 321−325.
(37) Hunter, R. J.; White, L. R. *Foundations of colloid science*; Clarendon Press, Oxford University Press: Oxford [Oxfordshire]; New York, 1987.
(38) Ohshima, H. A Simple Expression for Henry's Function for the Retardation Effect in Electrophoresis of Spherical Colloidal Particles. *J. Colloid Interface Sci.* **1994**, *168* (1), 269−271.
(39) Johnson, P. R.; Sun, N.; Elimelech, M. Colloid transport in geochemically heterogeneous porous media: Modeling and measurements. *Environ. Sci. Technol.* **1996**, *30* (11), 3284−3293.
(40) Liu, D. Colloid deposition dynamics in flow through porous media: Role of electrolyte concentration. *Environ. Sci. Technol.* **1995**, *29* (12), 2963−2973.
(41) Derjaguin, B. V.; Landau, L. D. The theory of the stability of strongly charged lyophobic sols and the adhesion of strongly charged particles in solutions of electrolites. *Acta Physicochim. URSS* **1941**, *14*, 733−762.
(42) Verwey, E. J. W.; Overbeek, J. T. G. *Theory of the stability of Lyophobic Colloids*; Elsevier: Amsterdam, 1948.
(43) Elimelech, M.; Gregory, J.; Jia, X.; Williams, R. A. *Particle Deposition and Aggregation: Measurement, Modeling, and Simulation*; Butterworth-Heinemann: Oxford, 1995.
(44) Franchi, A.; O'Melia, C. R. Effects of natural organic matter and solution chemistry on the deposition and reentrainment of colloids in porous media. *Environ. Sci. Technol.* **2003**, *37* (6), 1122−1129.
(45) Elimelech, M. Predicting collision efficiencies of colloidal particles in porous media. *Water Res.* **1992**, *26* (1), 1−8.
(46) Adamczyk, Z.; Siwek, B.; Zembala, M.; Belouschek, P. Kinetics of localized adsorption of colloid particles. *Adv. Colloid Interface Sci.* **1994**, *48* (C), 151−280.
(47) Sposito, G. *The chemistry of soils*; Oxford University Press: New York, 1989; p 277.
(48) Zaman, A. A.; Tsuchiya, R.; Moudgil, B. M. Adsorption of a low-molecular-weight polyacrylic acid on silica, alumina, and kaolin. *J. Colloid Interface Sci.* **2002**, *256* (1), 73−78.